

E.YA. GLUSHKO

Institute of Semiconductor Physics
(41, Nauky Prosp., Kyiv 03028, Ukraine)

SPECTRUM AND OPTICAL CONTRASTIVITY OF AN OXIDIZED COMB-LIKE SILICON PHOTONIC CRYSTAL

PACS 78.20.-e, 78.40.Fy

A typical oxidized ternary photonic crystal – A/B/A/C N-periodic structure – is investigated analytically and numerically in the framework of the transfer matrix formalism. The influence of the oxidation on photonic gaps and the positions of perfect reflection areas for (SiO₂/Si/SiO₂/Air)_N structure is calculated with regard for a transformation of the widths of silicon oxide layers. It is shown that the intrinsic optical contrastivity has a non-monotone behavior during the process of oxidation of silicon in the case of p-polarized electromagnetic waves. The found results will allow one to determine the optimal regimes of oxidation to obtain the needed optical properties of a photonic material.

Keywords: photonic bandgap materials, photonic resonators, trapped modes, oxidation, reflection, transmission.

1. Introduction

The well known feature of photonic crystals, which are structures with the spatially periodic index of refraction, is the existence of bandgaps in their optical spectra [1]. The expressed bandgap structure of photonic spectra arises due to the ordered character of the interference of electromagnetic waves inside an ordered structure. It is worth to note that an analogy between the formation of a spectrum of electrons in a semiconductor and the spectrum of standing electromagnetic waves in a photonic crystal was realized just in the very first investigations devoted to photonic crystals [2], which had promoted understanding the phenomenon and a quick progress in this area. At the present time, the photonic crystals, mainly binary, have been widely investigated as perspective objects of optical technologies in computing, signal processing, telecommunication, sensing, *etc.* [1]. The further development of this area can be coordinated with more complicated ternary photonic structures, which attract attention of investigators due to their more extensive list of useful properties in comparison with binary analogs [3, 4]. Among other factors, the optical contrastivity C_{ext} is a property, which allows one to characterize the photonic structures. For a simple case of two contacting semiinfinite media with refractive indices n_1, n_2 , the system symmetry dictates an

expression like $C_{\text{ext}} = |n_1 - n_2|/(n_1 + n_2)$ describing the external optical contrastivity. For more complex systems with well-expressed intrinsic structure, like that of photonic crystals, the definition of C_{ext} used above should be modified. To characterize the general ability of a complicated photonic structure to create well-expressed gaps in the spectrum, we will proceed from the general definition of contrastivity of a multicomponent system given in [5, 6]. In previous works, we have introduced a comprehensive quantitative definition of internal optical contrastivity as the total gap weighed over the frequency region of optical transparency of all constituent materials A, B, C. The definition is based on the well-known fundamental property of more contrastive ordered systems to form wider gaps in the total internal reflection (TIR) region [5, 6]. Due to its general character, the introduced definition keeps its validity for structures with any number of different components. In view of the circumstance that “the more the internal contrastivity between constituents of an optical structure, the wider the relative gap in a photonic spectrum,” we have $C_{\text{int}} = \text{gaps}/(\text{gaps} + \text{bands})$ for the internal optical contrastivity, where the numerator contains the total width of bandgaps, which arise inside the TIR region of the given structure at a chosen angle of incidence. The denominator corresponds to the frequency or energy region of the optical transparency of the structure.

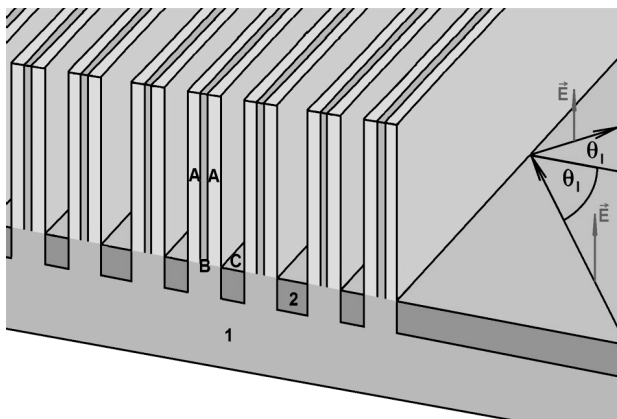


Fig. 1. A three-component $(A/B/A/C)_{N-1}(A/B/A)$ photonic crystal resonator as a part of the logic gate. 1, substrate; 2, protective antioxidizing layer, C, air voids, A, oxide layer, B, matrix material layer; θ_1 , angle of incidence of an external *p*-polarized plane wave

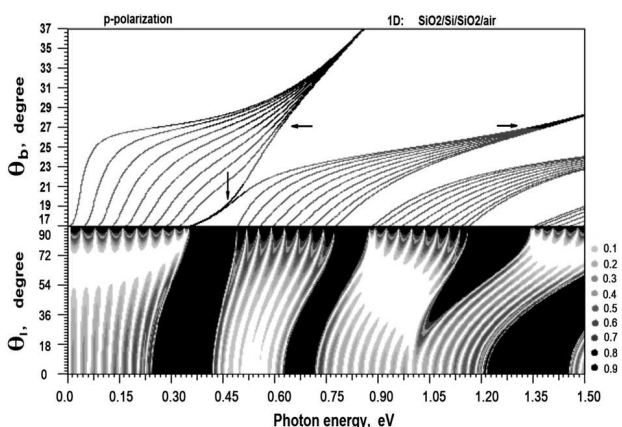


Fig. 2. Bandgap and reflection spectrum diagram of a ternary layered structure. θ_b panel: bandgap energy dependence of $(SiO_2/Si/SiO_2/Air)_{10}$ structure; θ_b , plane wave incidence angle inside the silicon B-layer, shown are $17^\circ < \theta_b < 90^\circ$; $b = 0.201 \mu m$, Si-layer thickness; $a = 0.339 \mu m$, thickness of air voids $c = 0.121 \mu m$; dielectric functions $\epsilon_a = 2.40$ and $\epsilon_b = 11.56$; horizontal arrows, boundary between transmitted (below) and waveguide modes (upper); vertical arrow, split local modes. θ_1 panel (below, right side: color gradation): angle-energy color diagram for the reflection of external incident light; θ_1 , plane wave external incidence angle $0^\circ < \theta_1 < 90^\circ$

In Fig. 1, a comb-like layered structure grown on substrate 1 and consisting of N periods of alternating from left to right materials A, B, A, and C with refractive indices n_a , n_b , and n_c . Protective layer 2

provides an opportunity to control the thickness of the A-layer using the oxidation process.

In this work, the influence of the oxidation on the internal optical contrastivity C_{int} and the positions of perfect reflection areas are investigated. It is shown that the oxidation can play a role of a technological mechanism to control the needed positions of separated bands and gaps in the optical spectra of silicon-based structures.

2. Bandgap Structure and Reflection Spectrum

The structure of the optical spectra of photonic crystals is important for applications in optoelectronic and all-optical devices. The distribution and the location of bandgaps in the spectrum, its dependence on the beam intensity and the incidence geometry may be used in the signal processing as a basic phenomenon to perform logic operations with signals. Therefore, the ternary photonic structures, being more complicated than binary structures, open wide perspectives in the creation of logic gate platforms with needed properties.

In Fig. 2, the calculated united bandgap structure and reflection spectrum diagram for a ternary layered 10-period $(SiO_2/Si/SiO_2/Air)_{10}$ photonic crystal are shown. In the upper θ_b panel, the photon energy dependences of the field band and local modes arising inside the total reflection region of $(SiO_2/Si/SiO_2/Air)$ structure in interval $17^\circ < \theta_b < 37^\circ$ are plotted, where θ_b are the wave angle in silicon B-layers. Here, to illustrate the better behavior of the band and local modes inside the TIR region, the energy interval was chosen a little wider than the silicon transparency region (0–1.0) eV. The thicknesses of the Si-layer, air voids, and the oxidized layer, are taken to be $b = 0.201 \mu m$, $c = 0.120 \mu m$, and $a = 0.339 \mu m$, respectively. The total internal reflection angle for silicon is $\phi_{TIR} = 17.105^\circ$. The high optical contrast manifests itself in relatively big photonic gaps and quickly narrowing bands in the depth of the TIR region. In a ternary structure, several kinds of band states may exist in dependence on a correlation between refractive indices n_a , n_b , n_c , and n_l . In the considered case where $n_c = n_l$, only two types of standing electromagnetic waves arise inside the TIR: waveguide modes existing in $SiO_2/Si/SiO_2$ walls and Si-sublayer waveguide

modes. The latter modes have falling field amplitudes beginning with silicon oxide on both sides, whereas the $\text{SiO}_2/\text{Si}/\text{SiO}_2$ wall modes begin the fall of their amplitudes in the C-voids. The horizontal arrows in the upper panel divide the angular space of the TIR region between the area of $\text{SiO}_2/\text{Si}/\text{SiO}_2$ waveguide waves $\theta_b < 27.13^\circ$ and the Si-layer waveguide area $27.13^\circ < \theta_b < 90^\circ$. One more kind of band states – transmitted modes, is absent in the considered case. They can exist only in filled comb structures when $n_c > n_l$.

Local states of two types – external and intrinsic relatively to layers A, may arise in an arbitrary ternary comb structure, which is placed in air. But only the intrinsic kind of local states exists, if material C is also air. In Fig. 2, the weakly detached A-intrinsic local states (vertical arrow) arise for the given geometry inside the first gap at $21.4 > \theta_b > 17.1$ degree and in the interval of photon energy between 0.338 and 0.488 eV. First signs of a twice degenerated local state exhibit themselves, when the thickness of A-layer begins to exceed 56.8 nm. At $a = 90$ nm, the local state arises also in the second gap. Then it vanishes there at approximately 250 nm and arises in the third gap at the approximately 900 nm-width of silicon dioxide. The local states of the external kind relatively to A-layer may exist only in a filled comb structure.

At the lower panel, the color angle-energy diagram of reflection is plotted. In general, the reflection diagram consists of the alternating regions of perfect reflection $R = 1$ and transmission windows with well-expressed modal structure. In our case of a ternary system, the total transmission band observed for silicon at the Brewster angle of incidence near $\theta_l = 72^\circ$ is suppressed here by existing A-layers of silicon dioxide.

Both diagrams, upper and lower, are matched in the area of whispering incidence at the angle of incidence $\theta_l \sim 90^\circ$, where sharp peaks of transmission transforms above into the resonator photonic modes of the TIR region.

It is worth to note that a difference exists between the positions of spectrum gaps inside the TIR region and the areas of perfect reflection usually observed at the normal incidence. In general, the regions of perfect reflection are wider than the matching gaps at $\theta_b \approx \phi_{\text{TIR}}$ for the p -polarization and narrower for the s -polarization. They are shifted toward the

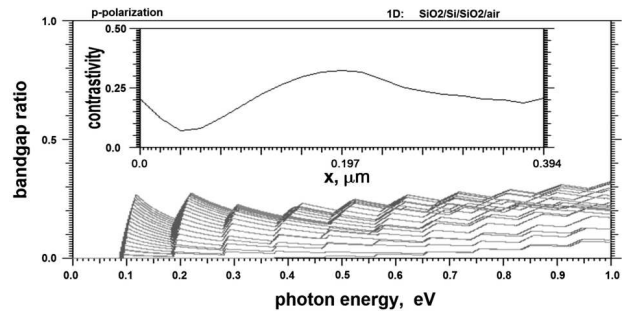


Fig. 3. $\text{SiO}_2/\text{Si}/\text{SiO}_2/\text{Air}$ periodic structure. Relative gap dependence on the photon energy. $b_0 = 1 \mu\text{m}$, $c_0 = 1 \mu\text{m}$. Inset: contrastivity C_{int} vs oxidation parameter x

long waves for both polarizations (Fig. 2, θ_l panel, p -polarization).

3. Oxidation

The initial non-oxidized structure has the thickness b_0 of every silicon layer and the thickness c_0 of air voids. Due to protective antioxidation layer 2 (Fig. 1), the system period $d_0 = b_0 + c_0$ remains constant during the process of oxidation. We assume in accordance with [7] that, for every unit thickness of silicon consumed, 2.27 unit thicknesses of oxide will appear during the oxidation process. Therefore, the following correlations between layer thicknesses are valid:

$$\begin{cases} a = 2.27x, \\ b = b_0 - 2x, \\ c = c_0 - 2.54x, \\ 2a + b + c = b_0 + c_0. \end{cases} \quad (1)$$

Depending on the etching temperature and the type of oxidation, wet or dry, the duration of the process may be as long as several hours [7] for the above-chosen parameters.

In Fig. 3, the calculated relative gap dependence on the photon energy is shown for $(\text{SiO}_2/\text{Si}/\text{SiO}_2/\text{Air})_{10}$ structure with initial parameters $b_0 = 1 \mu\text{m}$ and $c_0 = 1 \mu\text{m}$. There are 21 curves, each corresponding to $x_i = ic_0/50.8$, $i = 0, 1, 2, \dots, 20$, in Fig. 3. The positive inclined parts of curves correspond to the gap contribution into the ratio $\text{gaps}/(\text{bands} + \text{gaps})$, and the negative inclinations – to bands.

Both contributions of bands and gaps into the ratio $\text{gaps}/(\text{bands} + \text{gaps})$ were calculated inside the energy interval of transparency of silicon (0–1.0) eV along the $\theta_b = \phi_{\text{TIR}}$ line near the boundary of

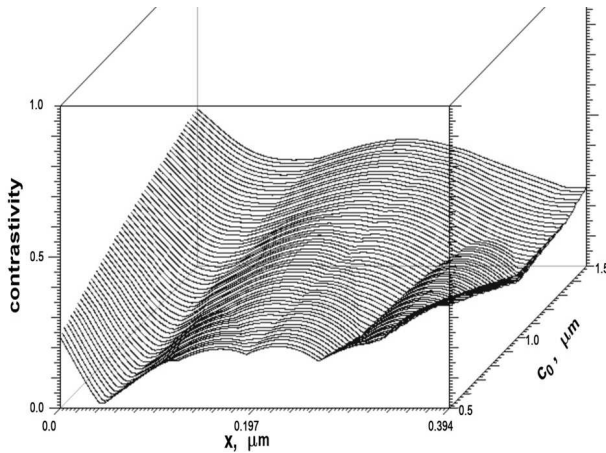


Fig. 4. Contrastivity C_{int} dependence of the parameter x on the initial thickness of air voids c_0 for p -polarized light in $\text{SiO}_2/\text{Si}/\text{SiO}_2/\text{Air}$ periodic structure. Optical transparency region (0, 1 eV). $\varphi_{\text{TIR}} = 17.105^\circ$, C_{int} varies from 0.017 at $a = 0.093 \mu\text{m}$, $c_0 = 0.5 \mu\text{m}$ to 0.521 at $a = 0$, $c_0 = 1.5 \mu\text{m}$

whispering incidence. The resulting behavior of the contrastivity dependence on the oxidation parameter x is plotted in the inset, where the left-hand part of the curve corresponds to a non-oxidized silicon, whereas the right part of the inset, $x = 0.394$, corresponds to completely oxidized silicon in the considered system.

The contrastivity non-monotony observed in Fig. 3 is explained by the complicate character of the bandgap structure behavior during the process of oxidation: bands and gaps leave the region of transparency or arrive at this region with different velocities. With the growing oxidation, the p -polarized bands became wider, the gaps became narrower, and the spectrum shifts to shorter wavelengths. Our calculation shows that, at the same time, the s -polarized field demonstrates an almost opposite behavior: the bands became narrower, the gaps became wider, but the spectrum is also blue-shifted.

The photonic bandgap structure at a given d_0 depends strongly on the oxide layer width a . Therefore, the oxidation may serve as a technological mechanism to prepare samples with the needed position of bands and gaps. This mechanism allows one to perform something like the sample adjustment to the needed laser frequency, by using the oxidation and different polarizations. So at $x = 0$, the first two photonic bands occupy intervals (0,

0.332) eV, (0.382, 0.689) eV for p -polarized waves (Fig. 2) and (0, 0.328) eV, (0.521, 0.750) eV for the s -polarization. Whereas the oxidation transfer to $x = 0.14934 \mu\text{m}$ ($a = 0.339 \mu\text{m}$, $c = 0.121 \mu\text{m}$, $b = 0.201 \mu\text{m}$) shifts the first two photonic bands to (0, 0.352) eV and (0.489, 0.774) eV for p -polarized waves and to (0, 0.266) eV and (0.551, 0.779) eV for the s -polarization.

4. Contrastivity

The intrinsic contrastivity determines the ability of an optical material to form gaps and reflection windows in the spectrum. Therefore, a non-contrastive medium should have a continuous spectrum of electromagnetic waves with the absence of gaps. We have calculated the optical contrast $x - c_0$ surface for the oxidized silicon periodic matrix $\text{SiO}_2/\text{Si}/\text{SiO}_2/\text{Air}$ with the starting thickness of the silicon layer $b_0 = 1.0 \mu\text{m}$. The result is shown in Fig. 4: the gap-band ratio was calculated in the region of optical transparency of Si for 60 different initial widths of air voids c_0 , which were changed in interval from $0.5 \mu\text{m}$ to $1.5 \mu\text{m}$. The surface has several ridges and valleys. The absolute minimum of $C_{\text{int}} = 0.017$ is found at $a = 0.093 \mu\text{m}$, $c_0 = 0.5 \mu\text{m}$, and the absolute maximum 0.521 is found at $a = 0$, $c_0 = 1.5 \mu\text{m}$. An intermediate maximum 0.420 is placed at $x = 0.219 \mu\text{m}$, $a = 0.497 \mu\text{m}$, $c_0 = 1.5 \mu\text{m}$. The weak contrastivity of the structure is a sign of narrow gaps and a band domination in the spectrum. On the contrary, the high magnitude of contrastivity shows a gap domination in the spectrum. A contrastivity map of such kind allows one to choose the initial geometry of a structure and the regime of oxidation to reach the demanded parameters.

5. Summary

In conclusion, the comprehensive quantitative definition of internal optical contrastivity as the total gap weighed over the frequency region of transparency is used to investigate the optical properties of silicon-based structures. It is shown that, proceeding from the obtained $x - c_0$ contrastivity map of a ternary $\text{SiO}_2/\text{Si}/\text{SiO}_2/\text{Air}$, an oxidized photonic crystal with the needed bandgap structure may be prepared. The study proves the high sensitivity of the photonic spectra of the silicon-based layered structures to the ox-

idation. Therefore, the controlled oxidation of prepared comb-like silicon photonic crystals may serve as an effective means to create optical media with predetermined properties.

1. S. John, D. Joannopoulos, S.G. Johnson, J.N. Winn, and R.D.Meade, *Photonic Crystals: Molding the Flow of Light* (Princeton Univ. Press, Princeton, NJ, 2008).
2. E. Yablonovich, *Phys. Rev. Let.* **58**, 2059 (1987).
3. S.K. Awasthi and S.P. Ojha, *Progress in Electromagnetics Research* **4**, 117 (2008).
4. X.Y. Dai, Y.J. Xiang, and S.C. Wen, *Progress in Electromagnetics Research* **120**, 17 (2011).
5. E.Ya. Glushko, *Opt. Commun.* **285**, 3133 (2012).
6. E.Ya. Glushko, *Eur. Phys. J. D* **66**, 36 (2012).
7. R.C. Jaeger, *Thermal Oxidation of Silicon. Introduction to Microelectronic Fabrication* (Prentice Hall, Upper Saddle River, 2001).

Received 31.01.14

Є.Я. Глушко

СПЕКТР ТА ОПТИЧНА
КОНТРАСТНІСТЬ ОКСИДОВАНОГО
ГРЕБІНЧАТОГО КРЕМНІЄВОГО
ФОТОННОГО КРИСТАЛА

Резюме

У роботі розглянуто типовий потрібний фотонний кристал – А/В/А/С N -періодична структура, оптичні властивості якої досліджувались аналітично і числовими розрахунками методом трансфер матриць. Вплив оксидизації на фотонні щілини та розташування проміжків абсолютно-го відбивання p -поляризованого світла розраховувався для $(\text{SiO}_2/\text{Si}/\text{SiO}_2/\text{Air})_N$ структури при різних N та з урахуванням змінної ширини прошарків оксиду кремнію. Показано, що внутрішня оптична контрастність структури монотонно змінюється протягом процесу оксидизації. Знайдені результати можуть бути корисні для визначення оптимальних режимів оксидизації з метою одержання фотонних матеріалів з потрібними властивостями.